Shaping Circularly Symmetric ADC Antennas by Combining Conic Sections for Amplitude and Phase Control at the Aperture

Adriano Z. F. Marques
Electrical Engineering Graduate Program (PPGEE)
Federal University of Minas Gerais (UFMG)
Belo Horizonte, Brasil
adrianozatti@ufmg.br

Fernando J. S. Moreira
Departament of Electronics Engineering (DELT)
Federal University of Minas Gerais (UFMG)
Belo Horizonte, Brasil
fernandomoreira@ufmg.br

2019 SBMO/IEEE MTT-S International Microwave and Optoelectronics Conference (IMOC) | 978-1-7281-3099-6/20/$31.00 ©2019 IEEE | DOI: 10.1109/IMOC43827.2019.9317633

***Abstract*—This paper presents a shaping technique for circularly symmetric ADC antennas for phase and amplitude control at the aperture. The method is iterative, using conic sections at each step to model the reflecting surfaces of the antenna. The system of equations is simple, using sine and cosine laws and conic equations. The solution at each step is obtained numerically, optimizing only a single variable. The technique is applied in two examples, one with uniform phase and amplitude aperture distribution, and the other with modeled phase and amplitude aperture distribution for a flat topped radiation pattern.**

Keywords—Reflector Antenna, ADC Antenna, Reflector Antenna Shaping.

I. Introduction

A similar shaping technique for circularly symmetric double reflector antennas by combining conic sections was presented in [1]. However, the previous technique [1] only allowed amplitude control at the antenna's aperture. The technique proposed in this paper goes further, also allowing phase control at the antenna's aperture. The system of equations developed does not present differential equations. it only uses sine and cosine laws, conic equations and the equation of reflection at conics. An iterative procedure is employed to determine the conics which locally represent the reflectors' generatrices. Each step provides a pair of conics by solving a non-linear set of equations. Figure 1 illustrates the conic representation of both reflectors.

The technique is applied in two examples of Axially-Displaced Cassegrain (ADC) antennas, but it can be adapted to other types of circularly symmetric double reflector antennas, like Axially-Displaced Gregorian (ADG), Axially-Displaced Ellipse (ADE) and Axially-Displaced Hyperbola (ADH) [1], by modifying the starting point of the antenna shaping. It can also be adapted to other circularly symmetric apertures' surfaces, not being restricted to flat ones.

The control of phase and amplitude at the aperture can model the radiation pattern of the antenna, like in one of the examples presented which provides a flat-topped beam with little ripples and side lobes. The other example presents a uniform phase and amplitude at the antenna's aperture.

II. Formulation

In the formulation, conic sections are used to represent the generatrices of the sub-reflector and the main reflector of the antenna. In each conic section, Snell's law of reflection is enforced, excluding the points of intersection between conic sections. The use of geometric optics limits the dimensions of this technique, forcing the sub-reflector to be at least ten times bigger than the wavelength for the proper control of the scattered field. The entire process takes less than a few seconds, and the biggest error found at a given step was one billionth of the wavelength.

At each step of the iterative method, a pair of conics is discovered, forming small pieces of the reflectors. Each step requires: the point on the aperture, which will be one of the conical foci, the phase at this point, and the power that will be focused at this point. The focal points at the aperture can be arbitrarily distributed, but are usually evenly distributed. The phase is determined directly in the equations through the path q to the aperture. The power over each of the foci can be determined by the conservation of energy that irradiates from the origin, reflects on the sub-reflector and the main reflector, and reaches the aperture. The equation of the power distribution was presented in [1], and is extended to the case where the power distribution at the aperture is discrete.

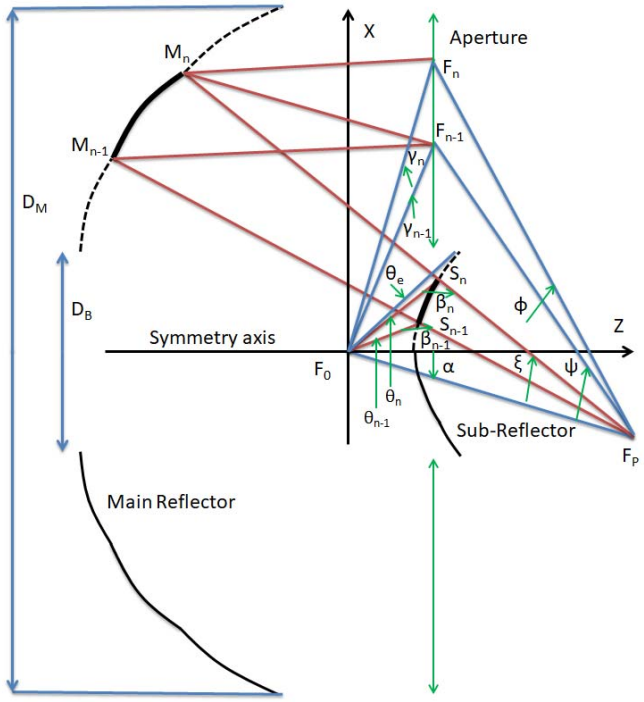

Fig. 1. ADC antenna shaping illustration.

A. Phase and Amplitude Control at the Aperture

The phase at the aperture is established in (1), adapting the wave equation of [2]:

$$e^{-jkq}, \tag{1}$$

This work was partially funded by CAPES/PROCAD 068419/14-01, CNPq and FAPEMIG.

where k is the propagation constant and q is the path of the wave that travels from the source, reflects at both reflectors and reaches the aperture. In the definition of the propagation constant in (2), c is the light speed, ω is the angular frequency, f is the frequency and λ is the wavelength:

$$k = \omega/c = 2\pi f/c = 2\pi/\lambda \quad (2)$$

The aperture's amplitude control is obtained by applying the conservation of energy that radiates from the source F_0 and reaches the aperture, as described in (3) and (4):

$$\int_0^{\theta_n} G_F(\theta_F)\, r_F^2\, sen\theta_F\, d\theta_F = N_F \int_{D_B/2}^{x_n} G_A(x)\, x\, dx \quad (3)$$

$$N_F = \int_0^{\theta_e} G_F(\theta_F)\, r_F^2\, sen\theta_F\, d\theta_F \,/\, \int_{D_B/2}^{D_M/2} G_A(x)\, x\, dx, \quad (4)$$

with $G_F(\theta_F)$ being the power density radiated by the source, $G_A(x)$ is the desired power density at the aperture, N_F being a normalization term to ensure that all the power radiated by the source and intercepted by the sub-reflector is conserved at the antenna's aperture, D_B is the diameter of the sub-reflector, D_M is the diameter of the main reflector and θ_e is the edge angle of the sub-reflector. For the case where the function $G_A(x)$ is discrete, with small variations of power density at the aperture, we have equations (5) and (6), with n_T being the number of foci over the aperture:

$$\int_0^{\theta_n} G_F(\theta_F) r_F^2 sen\theta_F\, d\theta_F = N_F \sum_{m=2}^{n} G_A(x_m)(x_m^2 - x_{m-1}^2) \quad (5)$$

$$N_F = \int_0^{\theta_e} G_F(\theta_F) r_F^2 sen\theta_F\, d\theta_F \,/\, \sum_{m=2}^{n_T} G_A(x_m)(x_m^2 - x_{m-1}^2) \quad (6)$$

B. Antenna Shaping

For the antenna shaping, we have used (7), (8), (13), (14), (18) and (19), obtained by trigonometric laws. Also, we have defined the parameters of the conics in (9), (10), (11), (12), (15) and (16), and have used the equation of reflection at conics in (17) obtained in [3] and the equation of the conics in polar coordinates in (20). Figure 1 illustrates the modeling.

The conic sections are black in Fig. 1, defined between points S_{n-1} and S_n for the sub-reflector, and M_{n-1} and M_n for the main reflector. The red lines represent the rays of the conics, and the blue lines the distances to the foci. The foci are symbolized by the letter F, where F_0 is the focus at the origin of the system, where the source is positioned, F_P the common focus of the conics of the sub-reflector and the main reflector, and F_{n-1} and F_n the foci at the aperture.

Thus, the unknown of the nonlinear system of equations (α) is defined as the angle between the z axis and the segment $\overline{F_0\, F_P}$. β_n is the angle between $\overline{F_0\, S_n}$ and $\overline{S_n\, F_P}$. θ_n is the angle between the z axis, and $\overline{F_0\, S_n}$. Also, γ_n is the angle between the z axis and $\overline{F_0\, F_n}$. At last, ξ, ψ and φ are defined as the angles between $\overline{F_0\, F_P}$, and $\overline{F_P\, M_n}$, $\overline{F_P\, F_{n-1}}$ and $\overline{F_P\, F_n}$.

The other variables of the nonlinear system of equations are q_n, q_{0P}, q_{Pn}, e_{0P} and e_{Pn}, being the major axis of the conics represented by the letter q, and the eccentricity by the letter e. The subscripts of these variables indicate the foci of the conic which they belong, like e_{0P} being the eccentricity of the conic with foci in F_0 and F_P. q_n is the sum of q_{0P} and q_{Pn}. Thus, the system is presented in (7) to (20).

$$\overline{F_0\, F_P} = \overline{F_0\, S_{n-1}}\, sin\, \beta_{n-1} / sin(-\alpha + \beta_{n-1} + \theta_{n-1}) \quad (7)$$

$$\overline{F_P\, S_{n-1}} = \overline{F_0\, F_P}\, sin(-\alpha + \theta_{n-1}) / sin\, \beta_{n-1} \quad (8)$$

$$q_{0P} = \overline{F_0\, S_{n-1}} - \overline{F_P\, S_{n-1}} \quad (9)$$

$$e_{0P} = \overline{F_0\, F_P}/q_{0P} \quad (10)$$

$$q_{Pn-1} = q_{n-1} - q_{0P} \quad (11)$$

$$q_{Pn} = q_n - q_{0P} \quad (12)$$

$$\overline{F_P\, F_{n-1}} = \sqrt{\overline{F_0\, F_{n-1}}^2 + \overline{F_0\, F_P}^2 - 2\, \overline{F_0\, F_{n-1}}\, \overline{F_0\, F_P} \cos(\alpha - \gamma_{n-1})} \quad (13)$$

$$\overline{F_P\, F_n} = \sqrt{\overline{F_0\, F_n}^2 + \overline{F_0\, F_P}^2 - 2\, \overline{F_0\, F_n}\, \overline{F_0\, F_P}\, cos(\alpha - \gamma_n)} \quad (14)$$

$$e_{Pn-1} = \overline{F_P\, F_{n-1}}/q_{Pn-1} \quad (15)$$

$$e_{Pn} = \overline{F_P\, F_n}/q_{Pn} \quad (16)$$

$$tan\frac{\xi}{2} = (e_{0P} + 1)\, tan\left(\frac{-\alpha + \theta_n}{2}\right) / (e_{0P} - 1) \quad (17)$$

$$cos\psi = (\overline{F_0\, F_P}^2 + \overline{F_P\, F_{n-1}}^2 - \overline{F_0\, F_{n-1}}^2) / (\overline{F_0\, F_P}\, \overline{F_P\, F_{n-1}}) \quad (18)$$

$$cos\phi = (\overline{F_0\, F_P}^2 + \overline{F_P\, F_n}^2 - \overline{F_0\, F_n}^2) / (\overline{F_0\, F_P}\, \overline{F_P\, F_n}) \quad (19)$$

$$error = \frac{(-1 + e_{Pn-1}{}^2)\, \overline{F_P\, F_{n-1}}}{2\, e_{Pn-1}\, (-1 + e_{Pn-1} \cos(\xi - \psi))} - \frac{(-1 + e_{Pn}{}^2)\, \overline{F_P\, F_n}}{2\, e_{Pn} (-1 + e_{Pn} \cos(\xi - \phi))} \quad (20)$$

With these equations, a numerical method is used to minimize the *error* of (20). This *error* represents in Fig. 1 a comparison of $\overline{F_P\, M_n}$ calculated with the conic of foci F_P and F_{n-1}, and $\overline{F_P\, M_n}$ of the conic of foci F_P and F_n. When *error* is zero, antenna continuity and the path q are established at point M_n.

At each step, $\overline{F_0\, S_{n-1}}$ and β_{n-1} are obtained from the previous iteration. The foci are initially given, q_n is obtained in (1) and θ_n is obtained in (3) and (4) or in (5) and (6).

After obtaining the value of α that minimizes the *error*, $\overline{F_0\, S_n}$ and β_n are calculated for the next iteration in (21) and (23). In addition, the points S_n and M_n that form the reflectors' surfaces are calculated in (22) and (25). These two points are defined by a module and an angle, using the notation in polar coordinates between parentheses:

$$\overline{F_0\, S_n} = \frac{\overline{F_0\, F_P}^2 - q_{0P}{}^2}{-2\, q_{0P} + 2\, \overline{F_0\, F_P} \cos(\alpha - \theta_n)} \quad (21)$$

$$S_n = (\overline{F_0\, S_n}, \angle\theta_n) \quad (22)$$

$$\beta_n = \pi + \alpha - \theta_n - \xi \quad (23)$$

$$\overline{F_P\, M_n} = ((e_{Pn}^{-1} - e_{Pn})\overline{F_P\, F_n})/(2 - 2\, e_{Pn}\, cos(\xi - \phi)) \quad (24)$$

$$M_n = S_n + (q_{0P} - \overline{F_0\, S_n} + \overline{F_P\, M_n}, \angle\beta_n + \theta_n) \quad (25)$$

III. Results

The shaping technique was applied in two cases. The first case is an ADC antenna with uniform aperture presented in [1] and the second one is a modeled phase and amplitude aperture distribution according to [4], with both cases illustrated together in Fig. 5 for comparison. The radiation patterns were generated using method of moments, and are presented in Fig. 3 for the uniform aperture and in Fig. 4 for the modeled aperture distribution. In these figures, the radiation patterns generated by the shaped antennas are compared to the ones presented in [1] and [4].

A. ADC Antenna with Uniform Aperture Distribution

The dimensions of the antenna are those presented in [1]. Thus, D_M = 6m, D_B = 0.6m, q = 3m, θ_e = 30º and the aperture is positioned at the z=0 plane. The operating frequency is 5GHz, which makes $D_M \approx 100\ \lambda$. The reflectors are shaped to provide uniform phase and amplitude at the aperture. The source model is that of (26), with p = 83:

$$G_F(\theta_F) = \frac{1}{r_F^2}\ cos^{2p}\frac{\theta_F}{2} \qquad (26)$$

As observed in Fig. 3, the radiation pattern of the shaped antenna is the same as in [1], showing that this technique works for this type of aperture.

B. ADC Antenna with Modeled Aperture Distribution

For the modeled aperture distribution, we have used the phase and amplitude distribution presented in [4]. However, the aperture presented in [4] is small in terms of wavelengths, being close to 10 λ, and has no blockage. Thus, the aperture used in this paper was similar to the previous example (uniform ADC) with amplitude and phase control starting at D_B and ending at D_M as illustrated in Fig. 2.

In order to compare the results of [4] with the presented shaped antenna, the radiation patterns were normalized. Thus, they do not represent the same radiated power value for the same gain.

Due to the differences between the apertures of [4] and this work, the radiation patterns present differences. However, the results obtained are relevant because of the similarities between the two radiation patterns. As shown in Fig. 4, the shaped antenna presented a flat-topped beam with small ripple in the center and was more directive because it was comparatively larger in wavelengths. In addition, it presented greater ripple and side lobes compared to [4], due to the blockage at the center of the aperture.

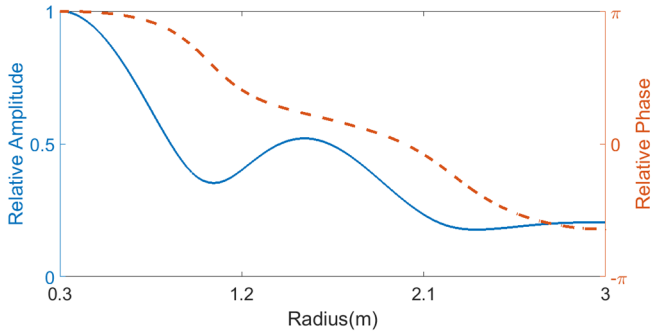

Fig. 2. Modeled aperture amplitude and phase pattern

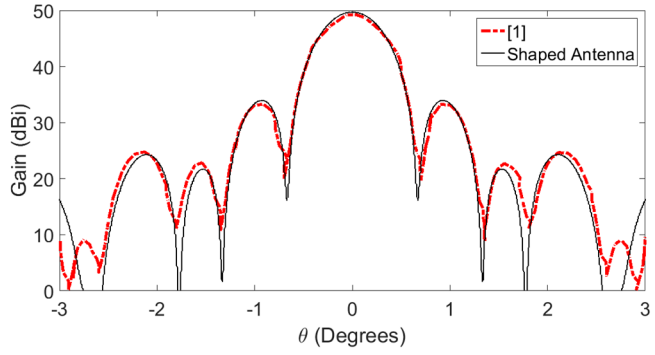

Fig. 3. Radiation pattern of the shaped antenna with uniform aperture compared to [1]

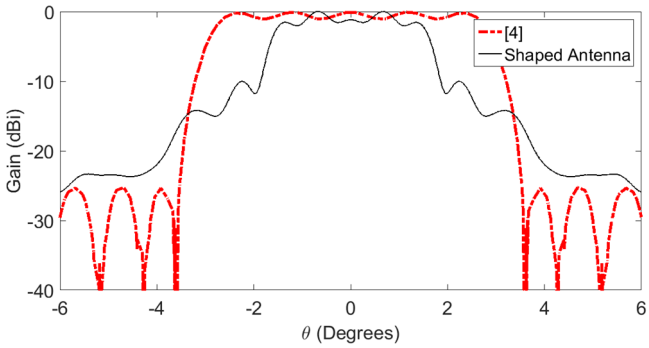

Fig. 4. Radiation pattern of the shaped antenna with modeled aperture compared to [4]

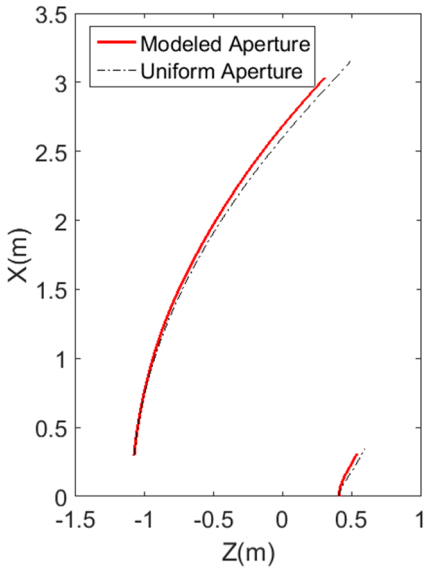

Fig. 5. ADC antennas generator for uniform and modeled apertures

IV. Conclusions

The technique presented has great use for dual-reflectors antenna projects, providing phase and amplitude control at the aperture. This control allowed antenna designs with different radiation patterns, as shown in Fig. 3 and Fig. 4.

The use of conic sections simplified the equations set. Hence, it does not presented differential equations, only trigonometric laws and conic equations.

This technique can also be used in other types of antennas, like ADG, ADH and ADE, in addition to the ADC considered in this paper. It can also be used with other shapes of apertures, not being limited to flat ones.

Acknowledgment

The radiation patterns were generated by Tcharles Faria.

References

[1] Fernando J. S. Moreira and José R. Bergmann, "Shaping Axis-Symmetric Dual-Reflector Antennas by Combining Conic Sections", IEEE Transactions On Antennas And Propagation, Vol. 59, No. 3, March 2011

[2] C. A. Balanis, "Antenna Theory Analysis and Design" 2nd Ed, New York, John Wiley & Sons, 1997, pp. 121-125.

[3] B. S. Westcott, "Shaped Reflector Antenna Design", New York, Research Studies Press, 1983, pp. 15-21.

[4] R. S. Elliott and G. J. Stern, "Shaped patterns from a continuous planar aperture distribution", IEE Proceedings, Vol. 135, Pt. H, No. 6, March 1988